We are IntechOpen,
the world's leading publisher of
Open Access books
Built by scientists, for scientists

6,900
Open access books available

185,000
International authors and editors

200M
Downloads

154
Countries delivered to

Our authors are among the

TOP 1%
most cited scientists

12.2%
Contributors from top 500 universities

BOOK CITATION INDEX
CLARIVATE ANALYTICS
INDEXED

WEB OF SCIENCE™

Selection of our books indexed in the Book Citation Index
in Web of Science™ Core Collection (BKCI)

Interested in publishing with us?
Contact book.department@intechopen.com

Low Cost Compact Multiband Printed Monopole Antennas and Arrays for Wireless Communications

Qi Luo, Jose Rocha Pereira and Henrique Salgado

Additional information is available at the end of the chapter

1. Introduction

Compact size printed multiband monopoles are of interest for a variety of applications such as WLAN, RFID and mobile terminals. If the antennas can be fabricated with a planar structure using PCB techniques, the cost can be kept low and the fabrication process is greatly simplified.

It is well-known that the size reduction will decrease the radiation efficiency of the antenna especially when its size is very small compared to the free space wavelength at its lowest resonant frequency. Conventional high permittivity substrates can be employed to reduce the size of the microstrip antenna (e.g. printed microstrip patch) but raises other design issues. When using this approach the bandwidth of the antenna is decreased and the surface wave propagations are excited, which can lead to the scan blindness if a beam-steerable phased array is built based on this antenna element. Therefore, it is important to investigate techniques for the design of compact and low cost microstrip antennas with promising radiation characteristics.

This chapter discusses various techniques of designing low cost, small-size printed monopole antennas and it is organized as follows. In section 2, antenna miniaturization techniques, based on fractal geometries and the use of lumped elements into the radiating element are discussed. In section 3, a low cost multiband printed planar monopole for mobile terminals is presented. This printed monopole exhibits five resonant frequencies and covers the desired frequency bands for mobile, WiMax and WLAN operations. Then in section 4, the design of a small size printed monopole array is addressed and two examples are given, one of which can be employed to increase the gain of the antenna and the other is suitable for MIMO applications of portable devices. Finally, recent developments in the field of low cost compact printed monopoles and arrays are discussed in section 5.

2. Compact and electrically small printed multiband monopoles

The currently available and future commercial wireless systems require antennas having wide bandwidth to support higher data rate and be able to operate at multiple frequency bands defined by various protocols. Compact size printed monopole antennas are important for the wireless applications due to its advantages of easy fabrication, omnidirectional radiation and wide operation bandwidth.

It is known that to reach the resonant condition, the dimension of the antenna must be a fraction of the wavelength at its resonant frequency. This means that the lower resonant frequency is, the larger the size of the antenna will be. From the limitations of the electrically small antennas defined by Chu [1], it is clear that antennas of smaller size always exhibit a higher quality factor whereas the bandwidth of an antenna is inversely proportional to the quality factor. As such the size reduction of an antenna will lead to the deterioration of its radiation performance. Therefore, compact multiband antenna design with promising radiation performance has attracted much research interests.

To be a low cost solution, it is desirable to fabricate the monopoles in PCB technology using only a single layer of substrate and a planar structure. Being a planar structure, the radiating element must have a geometry that can excite higher modes within a limited volume, to have a multiband operation. One approach that can be employed is to use fractal geometries to design compact multiband printed monopole antennas. Fractal geometry is a family of geometries that have the characteristics of inherent self-similar or self-affinity, which were used to describe and model complex shapes found in nature such as mountain ranges, waves and trees [2]. Recently, fractal techniques have been brought to the field of electromagnetic theory, a research field which has been called fractal electrodynamics; it has also been implemented in antenna design and named "fractal antenna engineering". This topic has been attracting much research interest. There are several advantages of using fractal geometries. First of all, it can reduce the size of the antenna, which makes it a good candidate for antenna miniaturization. Fractal geometries are self-filling structures that can be scaled without increasing the overall size. This characteristic provides opportunities for antenna designers to explore new geometries suitable for small antenna design. Secondly, fractal is a geometry that is self-repeated at different scales, which means that the fractal technique can be explored for designing antenna with multiple band operation and similar radiation patterns.

It is important to point out that although fractal geometries are self-filling structures that can be scaled without increasing the overall size, not all the geometries can contribute to the compact antenna design. Previous research found that some fractal geometries such as Hilbert and Peano curves, which exhibit a high degree of space filling, cannot effectively reduce the resonant frequency of the antenna due to the cancelling of the current between closely spaced lines [3].

2.1. Dual band fractal monopole

Studies show that Minkowski Island geometry is a good candidate for the design of multiband printed monopole antennas. Compared to other fractal geometries such as Hilbert curves, Minkowski Island geometry can work more efficiently with respect to the frequency reduction, due to its meandered-like configuration [3]. As demonstrated in Figure 1, when a Hilbert curve is employed to design a printed monopole antenna, the closely spaced lines can cause a large amount of current cancellation compared to the Minkowski Island geometry, which means that the effective electrical length of the Hilbert Curve antenna cannot benefit much from using such space filling geometry.

Input   Curre Cancells   Current Cancellation

(a)   (b)
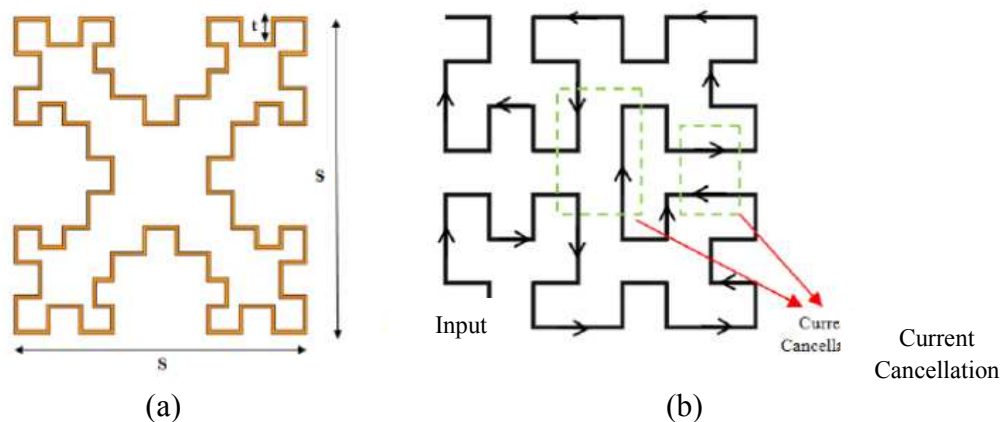
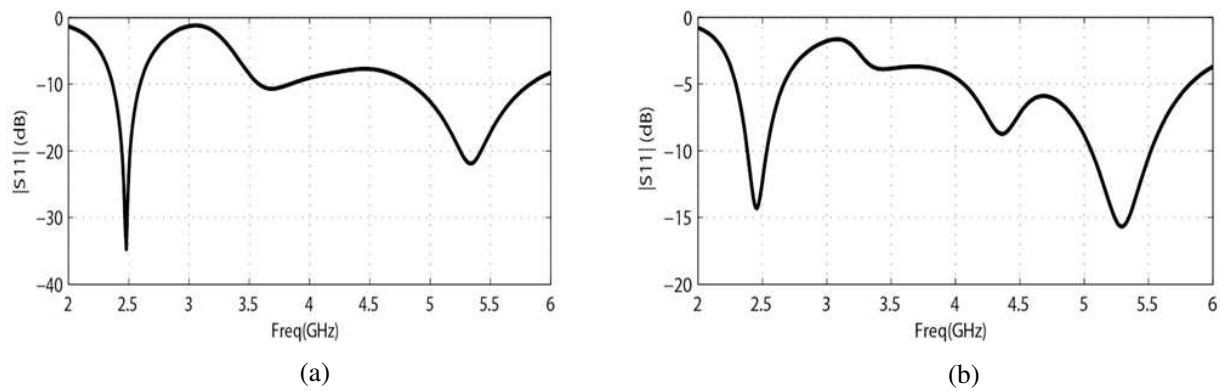**Figure 1.** (a) The 2nd iteration of Minkowski Island geometry; (b) current cancellation of a Hilbert Curve (b) [3].

In [4], two compact dual-band printed fractal monopoles for WLAN applications were presented. These two monopoles are designed using the 1st and 2nd iteration of the Minkowski Island, as presented in Figure 2. Figure 2(a) shows the printed monopole based on the 1st iteration Minkowski Island. Its size is 28 mm ×18 mm with a partial ground plane having a width of 35 mm and length of 10 mm on the back side of the substrate. The width of the microstrip line is 0.5 mm. Figure 2(b) shows another proposed fractal monopole using the 2nd iteration Minkowski Island. Its size is 21.5 mm ×18 mm and the size of the ground plane is 30 mm ×10 mm. The depth t, shown in Figure 1, is 1/4 of the side length (s/4) at each iteration for both antennas. The line widths of both antennas were set based on two factors: the antenna input impedance and the fact that the microstrip line needs to be narrow enough to avoid the intersection between adjacent lines. This issue is more significant for fractal of higher iterations. As a result of using a higher iteration fractal, narrower microstrip line needs to be used and the width of the microstrip line is reduced to 0.25 mm. Both of the proposed antennas are printed on the top side of the substrate, 0.813 mm thick Roger 4003 with relative permittivity ε_r=3.38, while the ground plane is printed at the bottom side. Behind the antenna elements, there is no ground plane.

Both of the proposed monopole antennas have a compact size compared to conventional printed monopole antennas, which need to have a length of approximately a quarter of
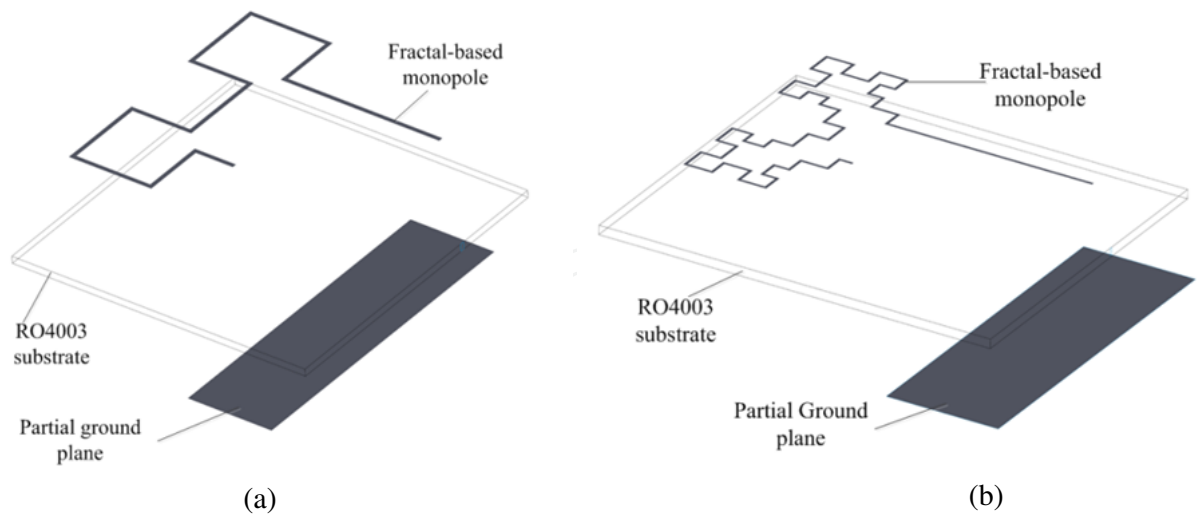
Figure 2. Exploded view of the fractal monopole antenna with geometry of: (a) 1st iteration Minkowski Island; (b) 2nd iteration of Minkowski Island proposed in [4].

wavelength. Moreover, it is found that without using any additional impedance matching techniques, both of these two proposed antennas exhibit good impedance match at multiple frequency bands, which is confirmed by the measurement results shown in Figure 3. These results show that the printed monopole of 1st iteration of Minkowski Island exhibits 10-dB return loss from 2.30-2.48 GHz, 3.3-3.7 GHz and 4.9-6.0 GHz, which covers the entire required frequency bands for 802.11a/b/g and WiMAX communications. For the 2nd iteration of Minkowski Island fractal monopole, the 10-dB return loss bands are 2.31-2.47 GHz and 5.0-5.5 GHz, which covers the two desired frequency bands for WLAN 802.11b/g standards.

Figure 3. Measured reflection coefficient of the proposed antenna with the: (a) 1st iteration and (b) 2nd iteration of Minkowski Island geometry [4].

The measured results also show that the radiation patterns at the H-plane are almost isotropic and in the E-plane they exhibit broadside radiation patterns, as expected. The measured maximum gain is around 1.5 dB at 2.45 GHz and 2.3 dB at 5.2 GHz for both antennas. According

to the simulation results, the radiation efficiency is 94% and 88% at 2.45 GHz, 97% and 93% at 5.26 GHz for the printed monopole of 1st and 2nd iteration of Minkowski Island, respectively. From these results, it is found that although higher size reduction can be achieved using higher iteration of the fractal geometry, the bandwidth as well as the radiation efficiency also decreases. This should be considered as a trade-off between size reduction and antenna performance. Figure 4 shows the measured E-and H-plane radiation pattern of the printed monopole with 2nd iteration of Minkowski Island at its dual resonant frequencies. Measurements showed that both antennas have similar radiation patterns so the measurement results for the other prototypes (the printed monopole of 1st iteration of Minkowski Island) are not given to avoid repetition.

(a)   (b)

(c)   (d)
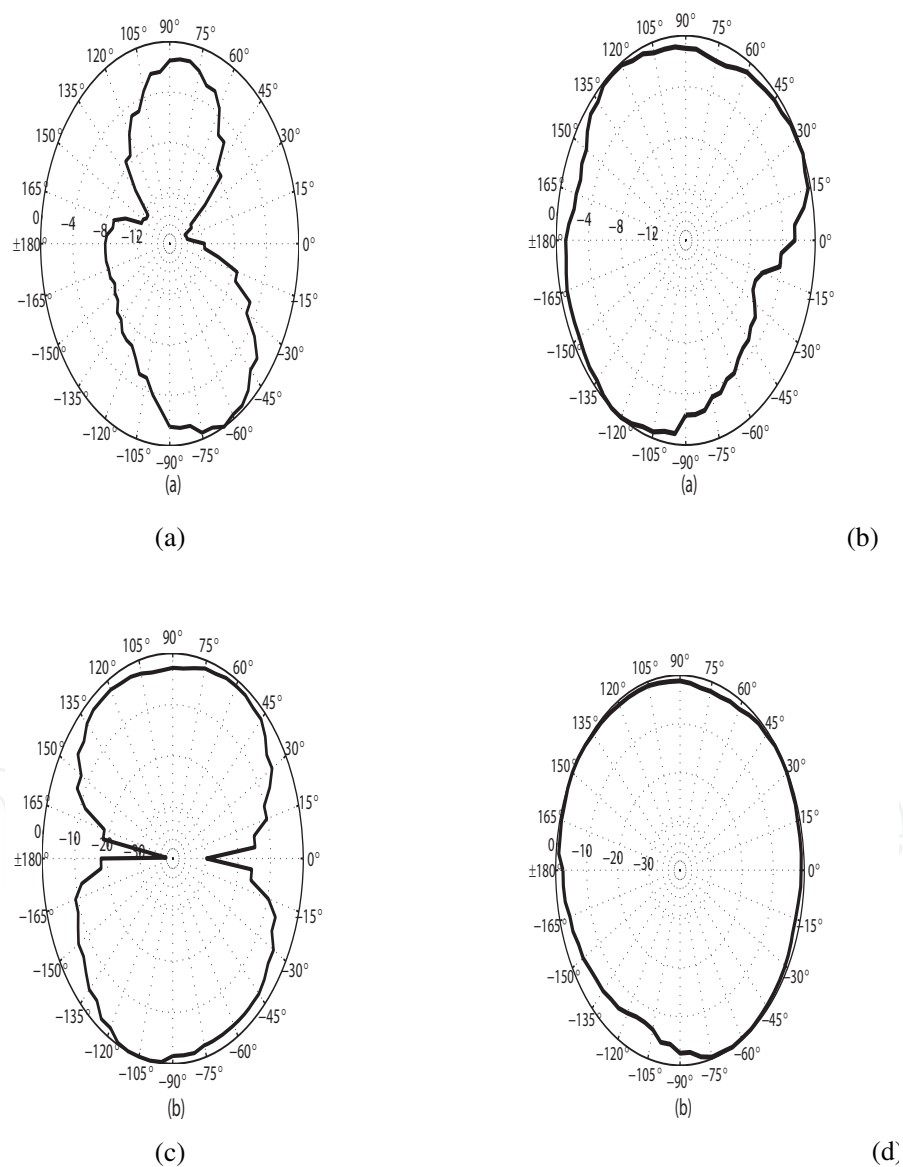
Figure 4. Measured radiation patterns of the proposed antenna with the 2nd iteration of Minkowski Island: (a) at 2.45°GHz, E-plane; and (b) at 2.45°GHz, H-plane; (c) at 5.3°GHz, E-plane and (d) at 5.3°GHz, H-plane [4].

2.2. Fractal ILA antenna

The frequency ratio of the multiband fractal antenna is investigated in [4]. It is shown that as a multiband antenna, the frequency ratio of the fractal antenna using the Minkowski geometry is nearly fixed. This indicates that in order to extend the fractal technique to other multiband antennas design, there is a need to explore an effective solution to overcome this limit. One technique that can be employed to extend the frequency ratio of the fractal-based multiband antenna design is to combine the fractal geometry with the meander line. One compact antenna suitable for a commercial wireless USB device is proposed by using such technique [5]. Since the objective is to design a printed fractal monopole antenna for WLAN USB dongle applications, based on the industrial requirement, the overall size of this antenna including the ground plane is chosen to be 20 mm×60 mm and the available space for antenna design is limited to no more than 20 mm × 10 mm.

A variation of the Koch fractal, which also can be referred as Cohen dipole fractal geometry, was used in this design. The Cohen dipole geometry, which is a variation of Koch fractal, was first proposed by Nathan Cohen [6] to design a dipole antenna with the feeding at the center position. Different from a conventional printed monopole antenna, the antenna radiating element is printed on the same layer of the ground plane. This type of antenna is named Inverted-L Antenna (ILA). As a typical printed monopole antenna, the antenna element with the feeding line and the ground plane are printed at the top and bottom side of the substrate, respectively. Meanwhile, the feeding port is located at the end of the substrate as shown in Figure 5. This might be a problem in a practical industrial design as other components, such as RF module, also need to be mounted on the same ground plane. Such problem can be solved by using ILA antenna.

Printed monopole   Antenna feeding point

Substrate

Ground plane
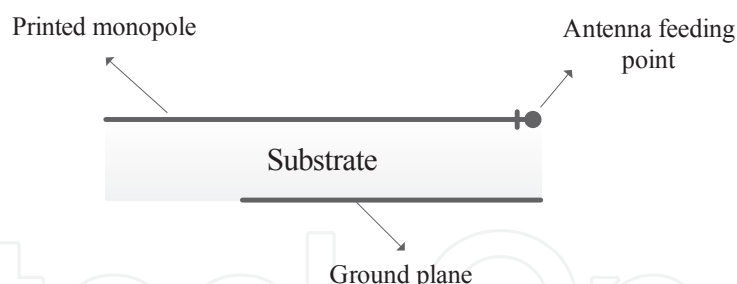
Figure 5. A typical configuration of the conventional printed monopole antenna

Figure 6 shows the exploded view of the proposed printed fractal ILA antenna in [5]. This antenna is designed on the Roger 4003 substrate with dielectric constant of 3.38 and thickness of 0.813 mm. The space occupied by the monopole antenna on the substrate is 10 mm ×20 mm and the size of the ground plane is 50 mm×20 mm, which is a typical size for a USB dongle. This structure was further optimized by doing numerical simulations in Ansoft HFSS to achieve a better impedance match at the required frequency bands. It is found that the size of the fractal geometry is critical in defining both the resonant frequencies while the existence of the horizontal microstrip line plays the role of adjusting the resonant frequencies to the desired region. Without the horizontal microstrip line, it is found that the proposed antenna can only exhibit resonances at around 2 and 6 GHz, which fails to cover the desired frequencies for

WLAN dual-band applications. However, adding the horizontal microstrip line with the appropriate length, the frequency ratio of the fractal antenna can be more controlled. After further optimization of the reflection coefficient over the desired frequency band, the width of the vertical microstrip line was chosen to be 1 mm and the width of the horizontal microstrip line was 0.5 mm. For the fractal, the width of the microstrip line was set to 0.35 mm.
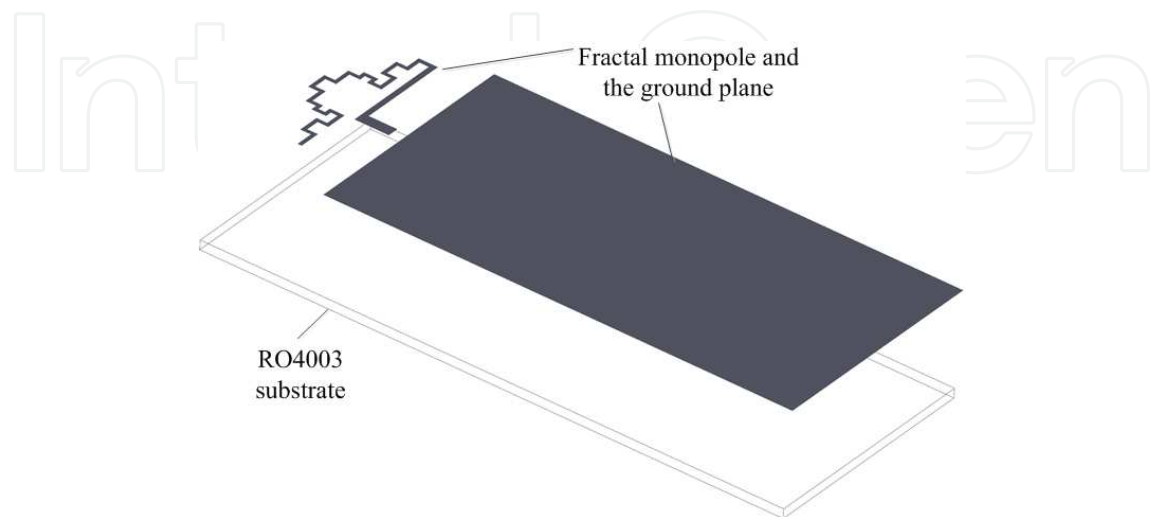
Figure 6. The exploded view of the printed fractal ILA antenna proposed in [5]

Figure 7 compares the reflection coefficient between simulation and measurement results. It can be seen that there is a good agreement between the simulated and measured reflection coefficient. The experimental result indicates that the proposed antenna has a S11<-10 dB with a bandwidth from 2.25 to 2.60 GHz and 5.06 to 5.62 GHz.
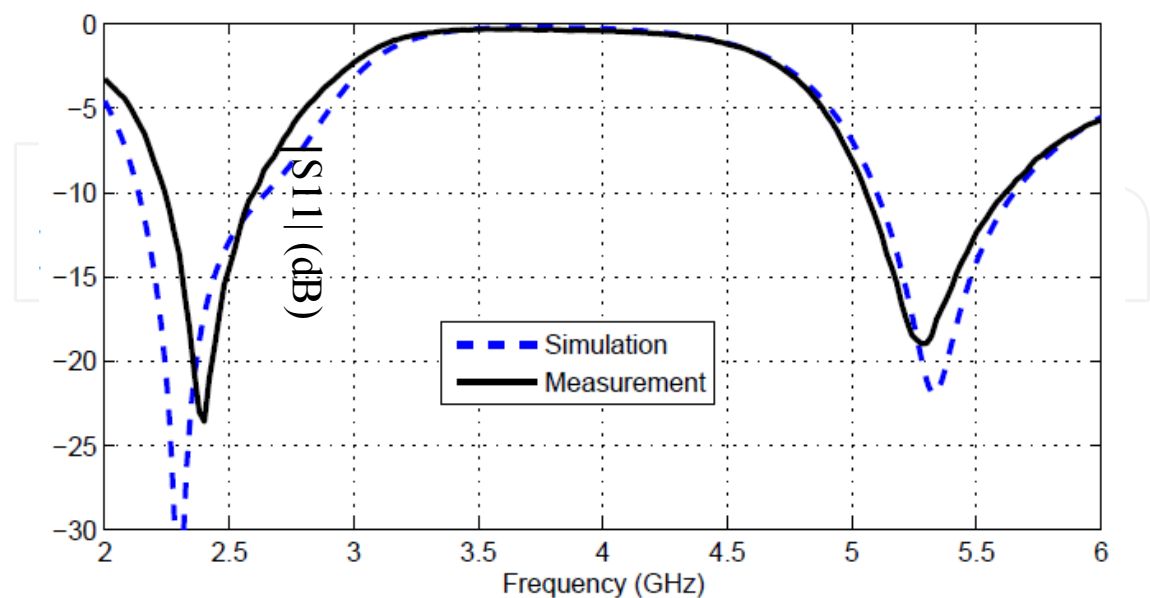
Figure 7. Comparison of the simulated and measured S11 of the fractal ILA in [5]

2.3. Compact Printed Monopole Antenna with Chip Inductor

Besides using fractal techniques to design printed monopoles of reduced size, another technique which can be employed is to introduce a lumped element, more specifically a chip inductor, into the antenna radiating element. In this way, the effective electrical length of the printed monopole is increased by the actual chip inductor instead of employing the fractal geometries that can bend a microstrip line of large length in a finite area.

Figure 8 shows the layout of the printed monopole antenna proposed in [7]. This antenna has a two-armed structure and for such monopole antenna the resonant frequency can be created by letting the overall length of each arm to be approximately a quarter of its effective wavelength on the substrate. The chip inductor is embedded in the middle of the left arm and generally speaking, the higher the value of the inductance, the lower the resonant frequency that can be achieved. However, increasing the inductance will also reduce the bandwidth and radiation efficiency of the antenna, which is the reason why a chip inductor with a higher inductance is not chosen in this study.

This antenna was printed on a Roger 4003 substrate with relative permittivity of 3.38 and thickness of 0.813 mm. The antenna and ground plane were printed on different sides of the substrate and there is no copper below the antenna section. The area of this antenna is only 10 mm ×10.5 mm, which is only 0.08 $\lambda_{2.4GHz}$ ×0.084 $\lambda_{2.4GHz}$, where $\lambda_{2.4GHz}$ represents the free space wavelength at 2.4 GHz. The higher band of the antenna is determined by the overall length L4+L5, which is approximately a quarter of a wavelength at 5.3 GHz. With the chip inductor, the overall length L1+L2+L3, which determines the lower band resonant frequency, is only 12.5 mm. This value is smaller than the length required for conventional monopole antennas. After adding the chip inductor, the resonant frequencies of the lower and higher band can be tuned by respectively changing the length of the arm L3 and L5, as demonstrated in the next section. By optimizing the length and width of each arm, this antenna is tuned to resonate at the desired frequencies. For more details about how to choose the value of the chip inductor and model it in the EM simulation software, readers can refer to [7].

The measured radiation patterns of the two-armed monopole antenna at 2.45 and 5.3 GHz show that the antenna has omnidirectional radiation patterns as a typical monopole antenna. Table 1 presents both measured and simulated results, as well as the calculated quality factor of the proposed monopole antenna. The quality factor was calculated based on the equations given below, taken from [8]:

$$Q(\omega_0) = \frac{2\sqrt{\beta}}{FBWv(\omega_0)}$$

$$FBWv(\omega_0) = \frac{\omega_+ - \omega_-}{\omega_0}$$

$$\sqrt{\beta} = \frac{s - 1}{2\sqrt{s}}$$

where the parameter s is the criterion for the maximum VSWR and ω_+, ω_-, ω_0 represent the higher frequency bound, lower frequency bound and central frequency of the antenna, respectively.
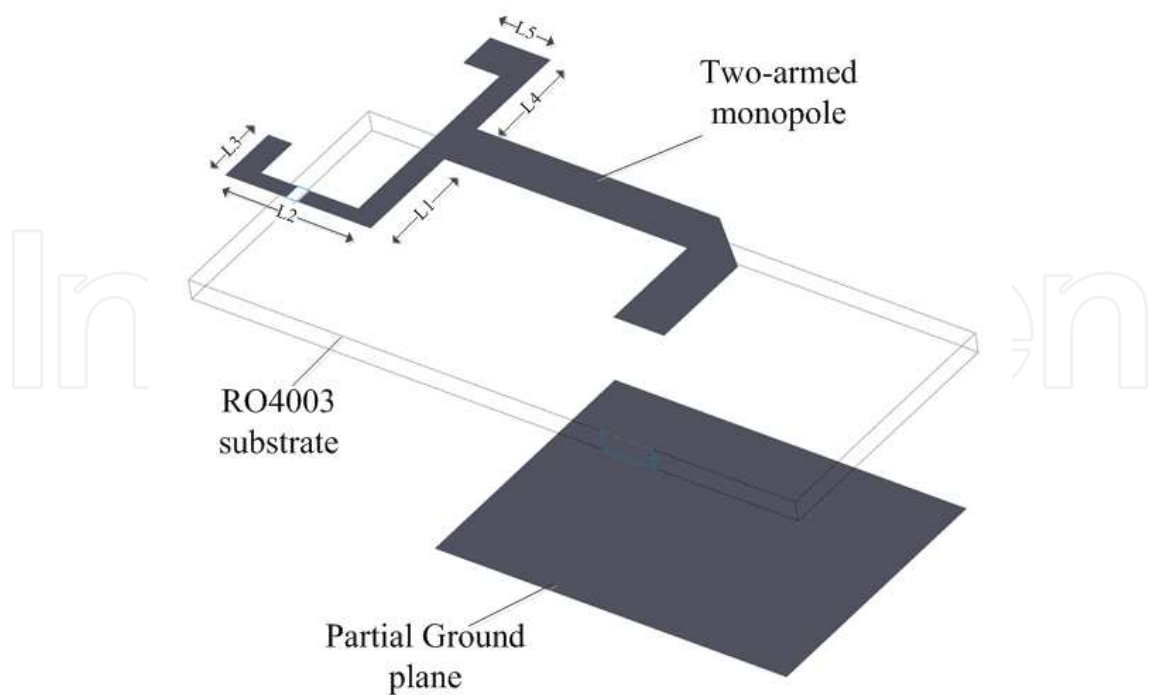
Figure 8. The configuration of the electrically small printed monopole antenna proposed in [7]

The lower bound of the quality factor (Q_{lb}) of the antenna was calculated by using the formula [8]:

$$Q_{lb} = \left[\frac{1}{(ka)^3} + \frac{1}{ka}\right]$$

From Table 1, it can be seen that the antenna has *ka* smaller than 0.5 and has a quality factor very close to its theoretical lower bound, where *a* is the radius of sphere that can enclose the maximum dimension of the antenna and *k* is the wavenumber.

| Properties	Proposed Antenna
Frequency (GHz)	2.45
Size (Wmm ×Lmm)	10×10.5
a (mm)	7.25
ka	0.37
Simulated Radiation efficiency (%)	72
Qlb	15.9
Measured 3:1 VSWR bandwidth (%)	5.10
Calculated Antenna Q	22.6

Table 1. Summary of performance of the proposed printed monopole antenna in [7]

## 3. Low cost printed planar monopole for mobile terminals

The rapid growth in mobile communications increases the needs of designing multiband internal antennas for mobile terminals. Meanwhile, it is also desirable to design such antennas as compact as possible. Planar Invert-F Antenna (PIFA) is one type of conventional antennas that has been widely employed in mobile phones. In [9, 10], two coupled-fed compact multiband PIFAs for wireless wide area networks (WWAN) were proposed for internal mobile phone antenna applications. The size reduction of these two antennas was achieved by shorting the antenna to the ground and bending the antenna structure. Printed monopole slot antennas and printed loop antennas have also been widely studied for multiband internal mobile phones. In [11, 12], two folded monopole slot antennas that can cover the penta-band WWAN operation were proposed for clam-shell mobile phones. These two antennas were designed by making several slots on the top of the ground plane. In [13-15], printed half-wavelength and meandered loop techniques were proposed for the design of multiband antennas for mobile handsets. However, all of these antennas have operating bands only covering GSM850/900 and DCS/PCS/UMTS bands, which are not enough for nowadays wireless communications. To make the antenna resonant at additional bands including Wireless LAN, one novel PIFA structure combining shorted parasitic patches, capacitive loads and slots was designed to support both quad-band mobile communication and dual-band wireless local area network (WLAN) operations [16]. Although this antenna can operate at several bands, it is extremely difficult to fabricate due to its complex structure. In [17], multiband operation including the WWAN and WLAN 2.4 GHz was achieved by cutting slots of different lengths at the edge of the system ground plane of the mobile phone. Operation in additional bands including GSM/DCS/PCS/UMTS/WLAN/WiMAX were achieved by cutting the loop-like slot on the top of the ground plane and shorting it to the ground plane [18]. However, shorting the antenna to the ground makes the resonant frequencies of the antenna vulnerable to the length of the ground plane. In fact the ground plane size used in [18] is smaller than the size of the system ground plane for a mobile phone. Other techniques have also been developed to design compact multiband antennas for wireless communications. In [19], a multiband antenna that can support WWAN and 2.4 GHz WLAN frequency bands was implemented by using a switchable feed and ground. In [20], a small size multiband antenna for wireless mobile system was designed based on double negative (DNG) zeroth order resonator (ZOR). However, it is noticed that these antennas have rather complex structures and they are quite difficult to fabricate. In [21], a chip inductor was embedded in the printed monopole antenna, which resulted in a compact antenna for mobile handset application.

One compact multiband printed monopole for mobile application has been recently presented in [3]. This design overcomes some of these limitations discussed above. Figure 9 shows the structure of the proposed antenna and the main dimensions of the antenna elements are given in Figure 10. The antenna element is printed on the top side of the substrate while the ground plane is located at the bottom side. Behind the monopole antenna, there is no ground. The chip inductor, of series Coilcraft 0402HP with an inductance of 20 nH, is embedded between the branch A and B as shown in Figure 10. This antenna has a multi-branch structure, each of which determines different resonant frequencies. The lowest resonant frequency, 960 MHz, is

determined by both the inductance of the chip inductor and the overall length of branch A and B. Although the chip inductor can also influence the resonant frequency at 1800 MHz to some extent, this resonance is mainly determined by the length of branch A. The overall length of branch D and the length of branch E determine the resonant frequencies at 2.4 and 5.2 GHz, respectively. The frequency band at 3.8 GHz is related to the length of branch C and the width of branch A.
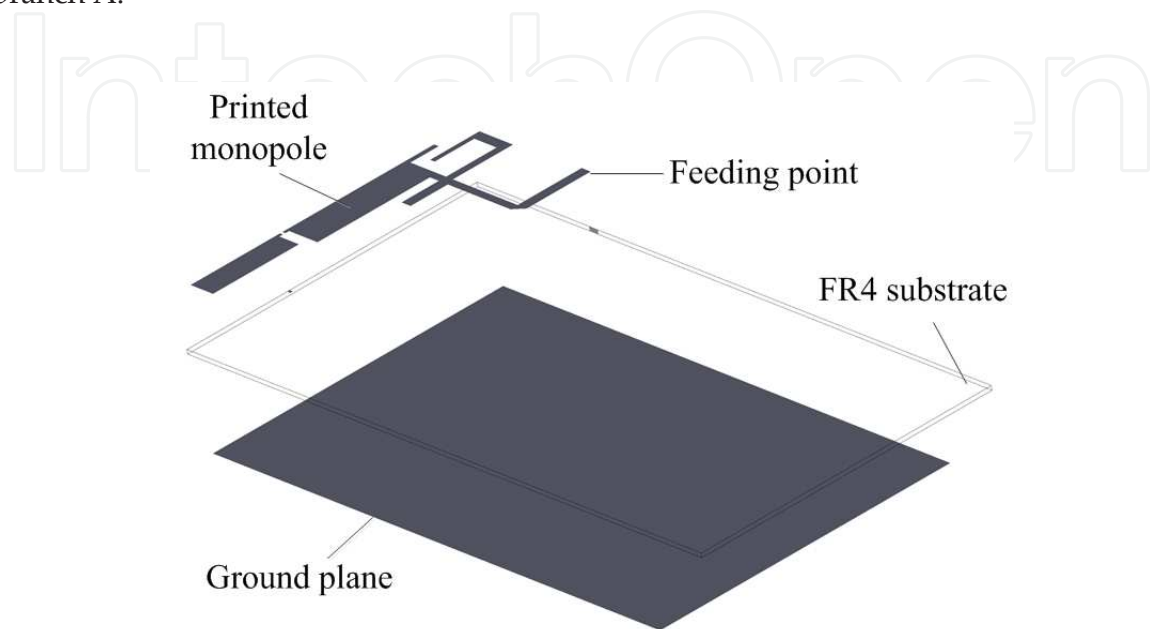
Figure 9. Structure of the multiband printed monopole antenna for mobile terminals [3]
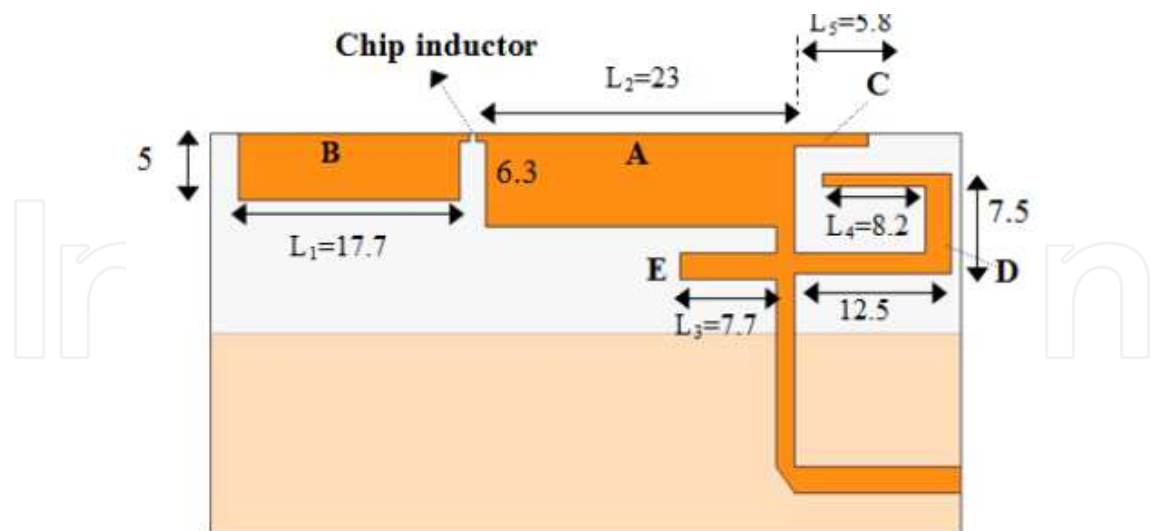

Figure 10. The main dimensions of the multiband printed monopole antenna [3]

This antenna is printed on the inexpensive substrate FR4 (relative permittivity of 4.4) with thickness of 0.8 mm and size 100mm ×60mm, which is a reasonable circuit board size for a PDA or smart phone device. To achieve a better impedance matching at each band, the length and

width of each branch of the antenna were optimized through numerical simulations. In the simulation set-up, the model of the chip inductor is built based on the studies presented in [7]. As stated before, the chip inductor mainly influences the first two lower frequency bands. In these two lower frequency bands, the value of the chip inductor is more critical in determining the lowest resonant frequency; as a result, in the simulation set-up, the equivalent inductance and series resistance of the chip inductor model were calculated at 960 MHz using the formulas provided in [7], and they are 20.6 nH and 2Ω, respectively.

Figure 11 shows the measured and simulated reflection coefficient of the proposed antenna. This antenna was measured using the network analyzer Agilent PNA E8363B. It can be observed that there is a good agreement between the measurement and simulation results. The experiment result shows that the proposed antenna has 3:1 VSWR bandwidth covering 860-1060 MHz, 1710-2067 MHz, 2360-2500 MHz, 3250-4625 MHz, 5080-5410 MHz, which includes almost all the required frequency bands for GSM900 (890-960MHz), DCS (1710-1880MHz), PCS (1850-1990MHz), UMTS (1920-2170MHz), WLAN dual band (2400-2484/5150-5350MHz) and WiMAX (3400-3600MHz) operations.
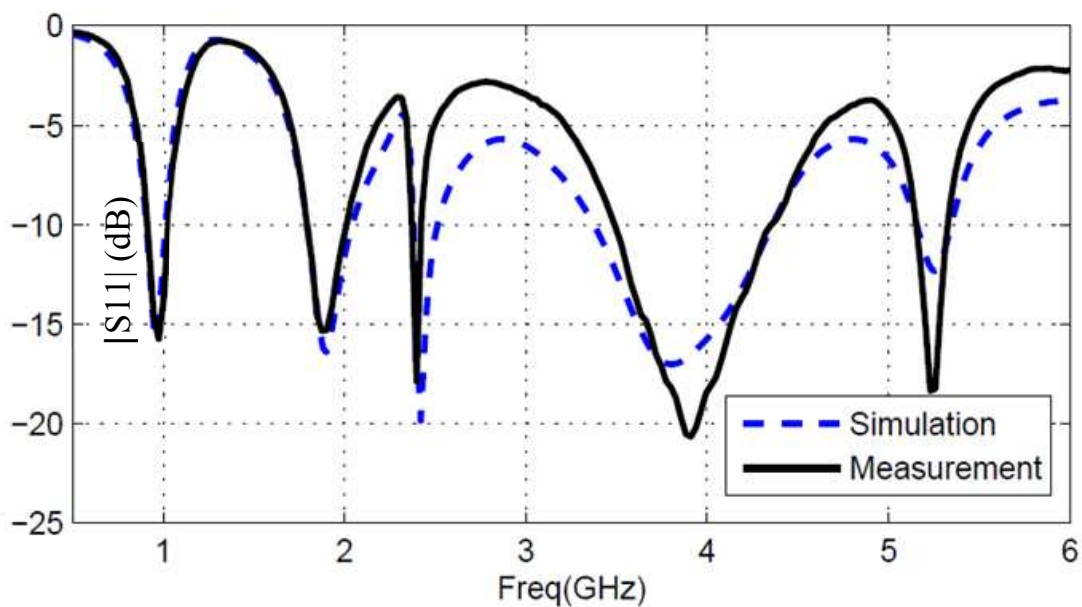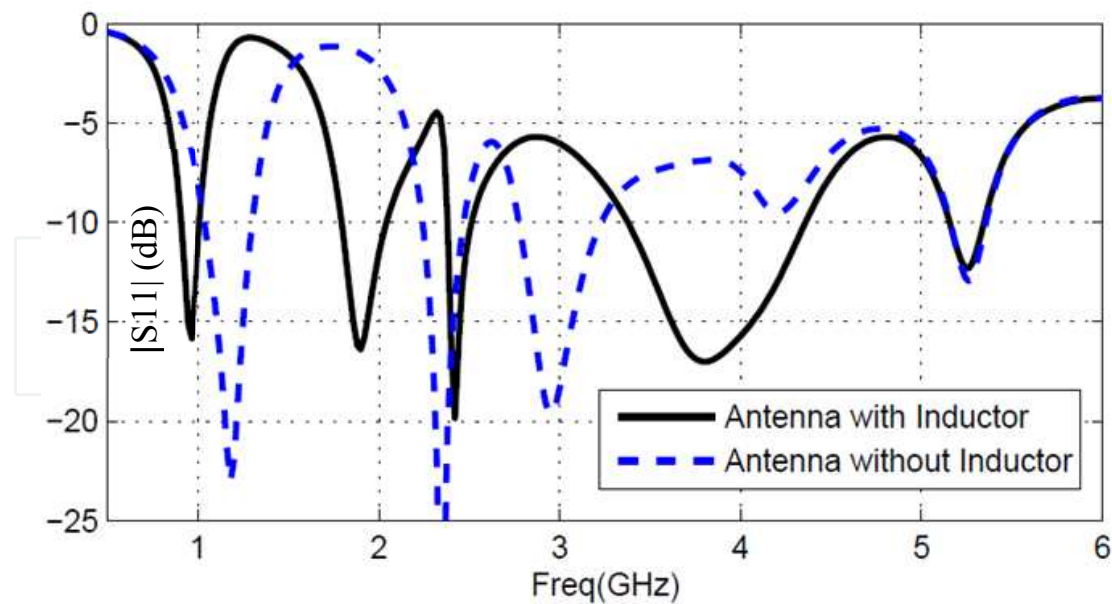

Figure 11. The measured and simulated reflection coefficient of the multiband printed monopole antenna [3]

Figure 12 presents the comparison of the simulated reflection coefficient between the proposed antenna with and without the embedded chip inductor. It is found that without the chip inductor, at the lowest frequency band the antenna can only resonate at around 1.1 GHz. After introducing the chip inductor, this resonant frequency reduces to 960 MHz and also brings down other higher modes to become resonant at 1.8 GHz. It is also observed that the chip inductor has little influence on the resonant frequencies at 2.4 and 5.2 GHz.

Figure 13 shows the simulated surface current distribution of the proposed antenna at each operation frequency. It is observed that at 960 MHz, there is a strong current on branches A

Figure 12. The comparison of the simulated reflection coefficient between the multiband printed monopole antenna with and without the embedded the chip inductor [3]

and B. At 1800 and 1900 MHz, the current is mainly distributed on branch B. It is also clear that branches D and E are responsible for the resonant frequency at 2.4 and 5.2 GHz, respectively. Regarding the resonance at 3.8 GHz, it is mainly determined by branch C and the coupling between branch C and D.

Besides being a completely planar structure, another advantage of the proposed antenna is that the size of the ground plane has little influence on its resonant characteristics compared to the designs that short the antenna structure to the ground plane. The proposed monopole antenna with different lengths of the ground plane has also been investigated. Figure 14 shows the simulated reflection coefficient of the proposed antenna with ground planes of different lengths. It was found that when decreasing the length of the ground plane, at the desired frequency bands the proposed antenna only exhibits small frequency shifts and some changes on the amplitude of the reflection coefficient.

The scenario in which the antenna is put into the center of a plastic housing box was also investigated in this work. In the simulation model, the wall of the plastic housing is 1 mm thick, 14 mm high and has a dielectric permittivity of 3.5. The simulation results (Figure 15) indicate that, compared to the case when the antenna is radiating in free space, there is almost no influence on the reflection coefficient of the proposed antenna except for a small frequency shift at the 3.8 GHz band, when within the plastic housing.

The measured radiation patterns of the proposed antenna in free space are presented in Figure 16. It is found that at all the desired frequencies the proposed antenna has radiation patterns similar to a typical monopole antenna, which normally has omnidirectional radiation patterns. The simulation results also suggest that the antenna has moderate gain and efficiency at its operation frequency bands. Table 2 summarizes the peak gain and radiation efficiency at the

desired frequencies. It is observed that at 5.2 GHz, the radiation efficiency is rather low compared to other resonant frequencies. This can be explained by the fact that there is a strong coupling between the branch **B** and **E** (see Figure 12) while the branch **E** is also very closed to the ground plane, with a negative impact on the radiation efficiency.
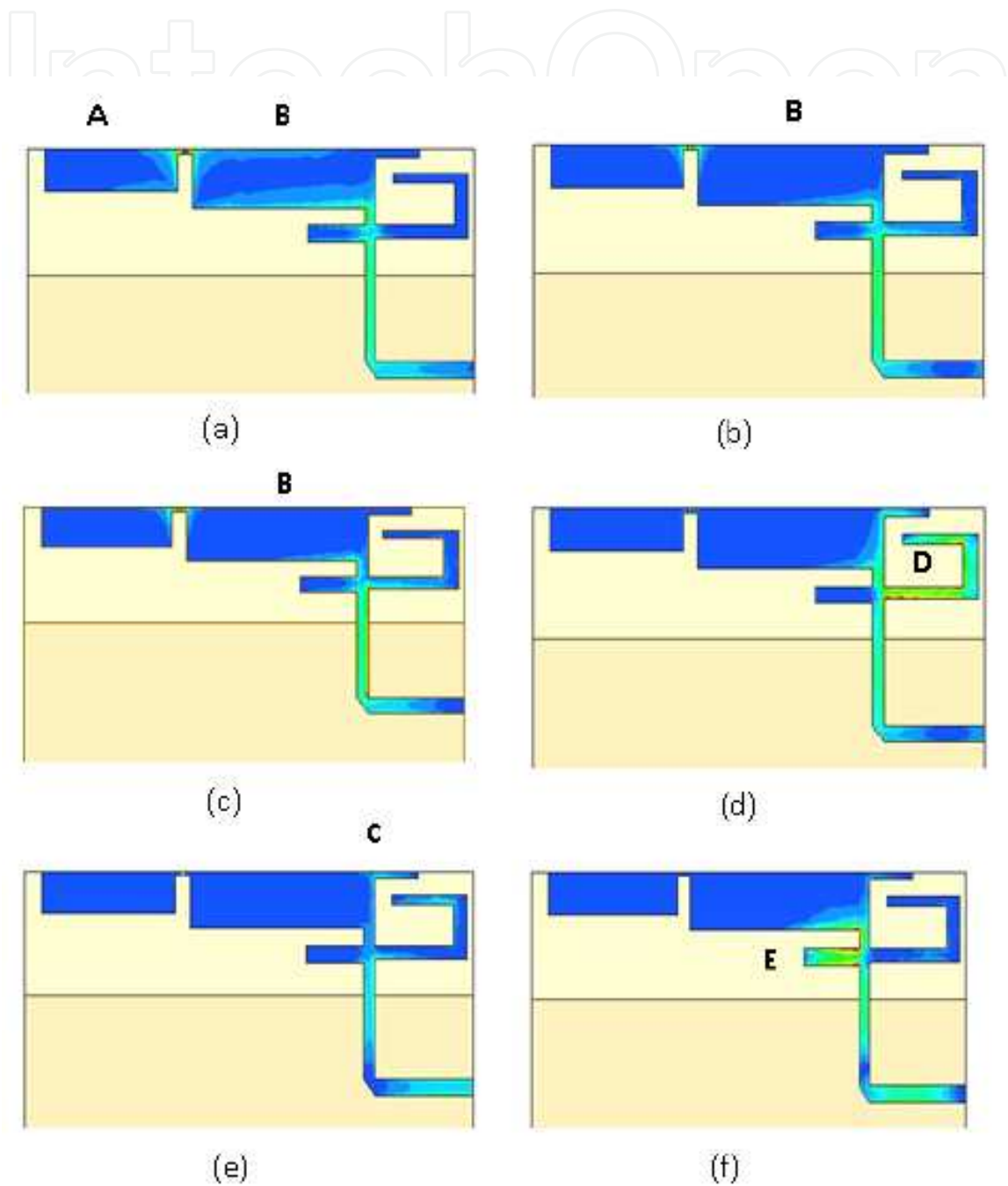
Figure 13. The simulated surface current distribution of the multiband printed monopole antenna [3] : (a) 960 MHz; (b)1800 MHz; (c)1900 MHz; (d)2.4 GHz; (e)3.8 GHz and (f)5.25 GHz. The stronger current is represented by lighter colors
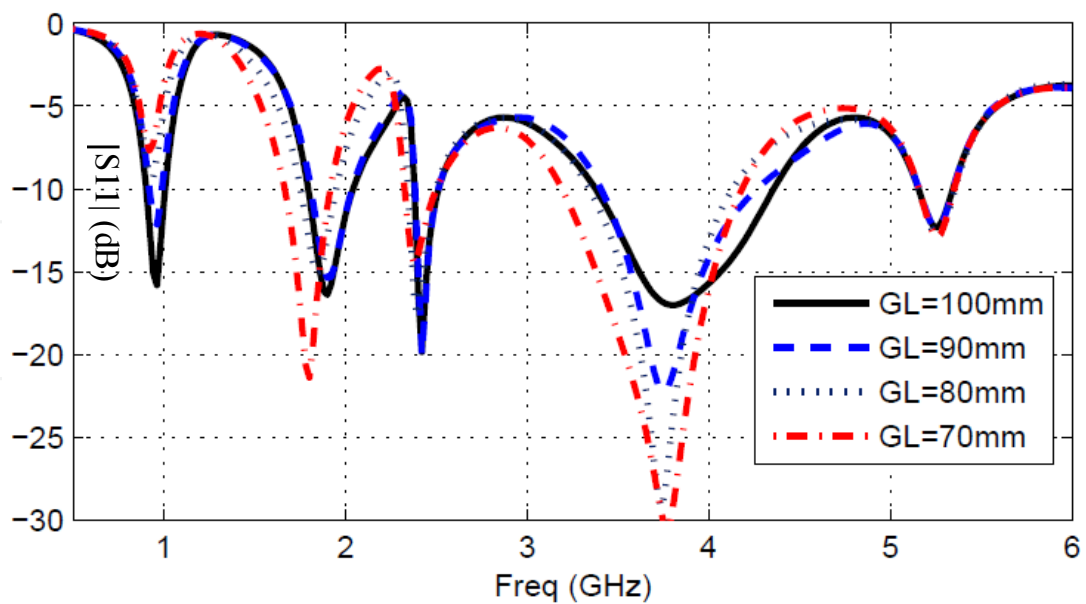
Figure 14. The simulated return loss of the multiband printed monopole antenna with ground planes of different lengths [3]
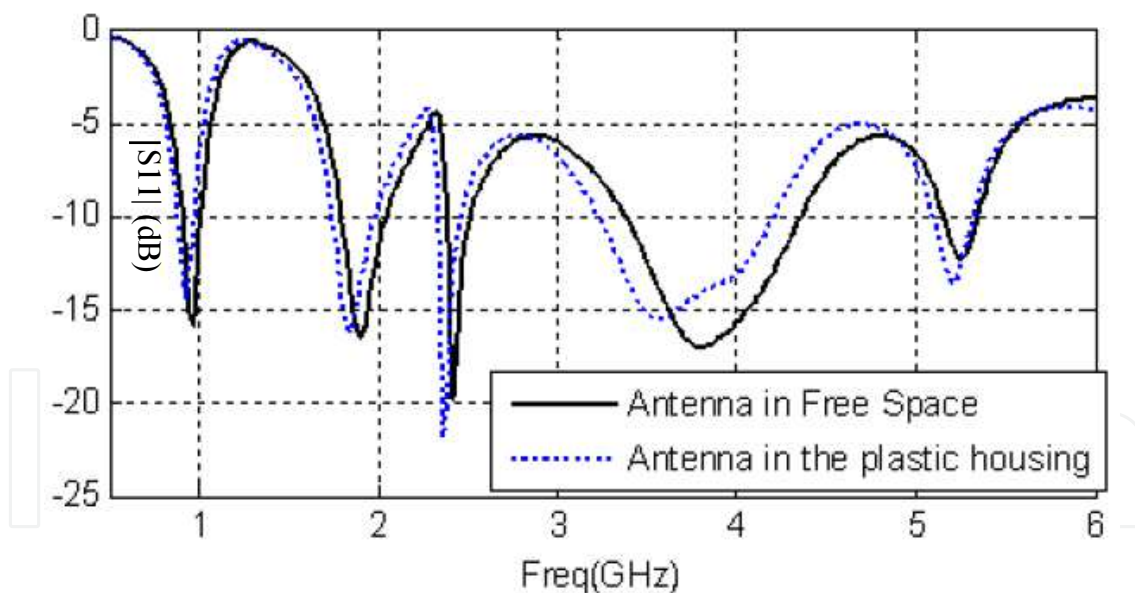

Figure 15. Comparison of the simulated S11 of the multiband antenna when placed in a plastic housing and in free space [3]

The Specific Absorption Ratio is also analyzed in this study. The simulation result indicates that the SAR value averaged over 1 gram of head tissue is 1.4 W/Kg, which meets the released SAR limitation of 1.6 W/Kg. It is expected that the SAR value in reality will be smaller than the simulated one due to the adding of the case for the mobile phones.

Frequency(GHz)	Simulated Peak Gain(dBi) / Radiation Efficiency
0.96	1.5 (93.7%)
1.8	2.6 (91.9%)
1.9	2.5 (92.2%)
2.4	2.7 (77.3%)
3.5	2.8 (86.8%)
5.2	1.7 (67.9%)

Table 2. Simulated Peak gain and radiation efficiency of the proposed antenna at each frequency band [3]
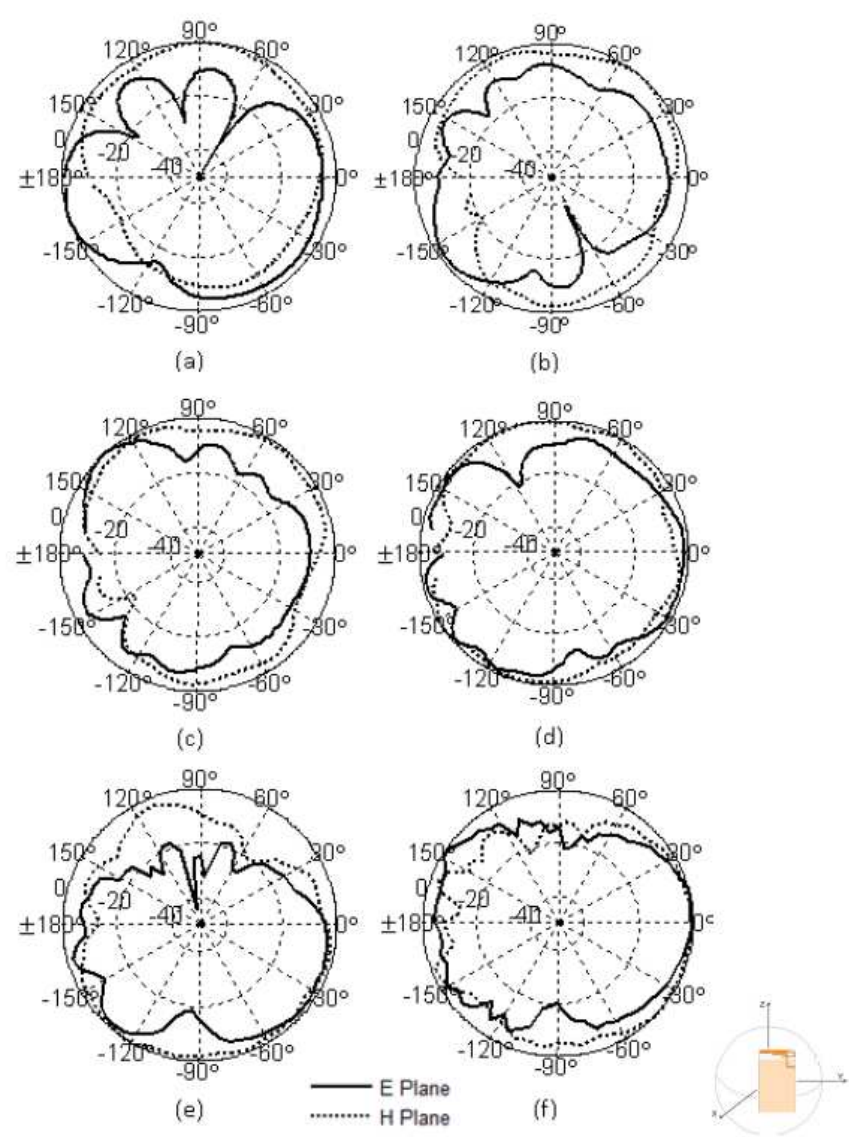

Figure 16. Measured E-plane (X-Z Plane) and H-plane (X-Y plane) radiation patterns of the proposed multiband antenna at: (a) 960MHz; (b) 1800MHz; (c) 1900MHz; (d) 2.4GHz; (e) 3.5GHz; (f) 5.2GHz [3]

4. Small size printed monopole array

4.1. Fractal monopole antenna array

To increase the directivity of an antenna system, the use of antenna arrays is an effective solution if an additional antenna element can be added in the wireless device. A single feed antenna array has the advantages of easy fabrication and does not need any extra RF compo‐ nents such has a phase shifter. It is desirable to design such antenna in a planar structure as it can simplify the fabrication process and reduce the fabrication cost. One compact single feed multiband printed monopole antenna array using the 2nd iteration of the Minkowski fractal geometry designed for WLAN dual band application is presented in [22].

The 2nd iteration of the Minkowski fractal geometry (see Figure 1) was chosen for this design due to its compact size. Figure 17 shows the geometry of the proposed fractal monopole array. This antenna was fabricated on a Roger 4003 substrate of thickness 0.813 mm and relative permittivity 3.38. The substrate is 112 mm long and 65 mm wide, which is the size for a typical PDA terminal. The antenna is constituted by two equal 2nd iteration Minkowski fractal monopoles fed by a single microstrip line of 1.89 mm wide. The line width of the fractal geometries is 0.25 mm and they are connected to the feed line by another horizontal microstrip line of width 1.2 mm. The partial ground plane is printed on the back side of the substrate and the antenna is printed on the top side.
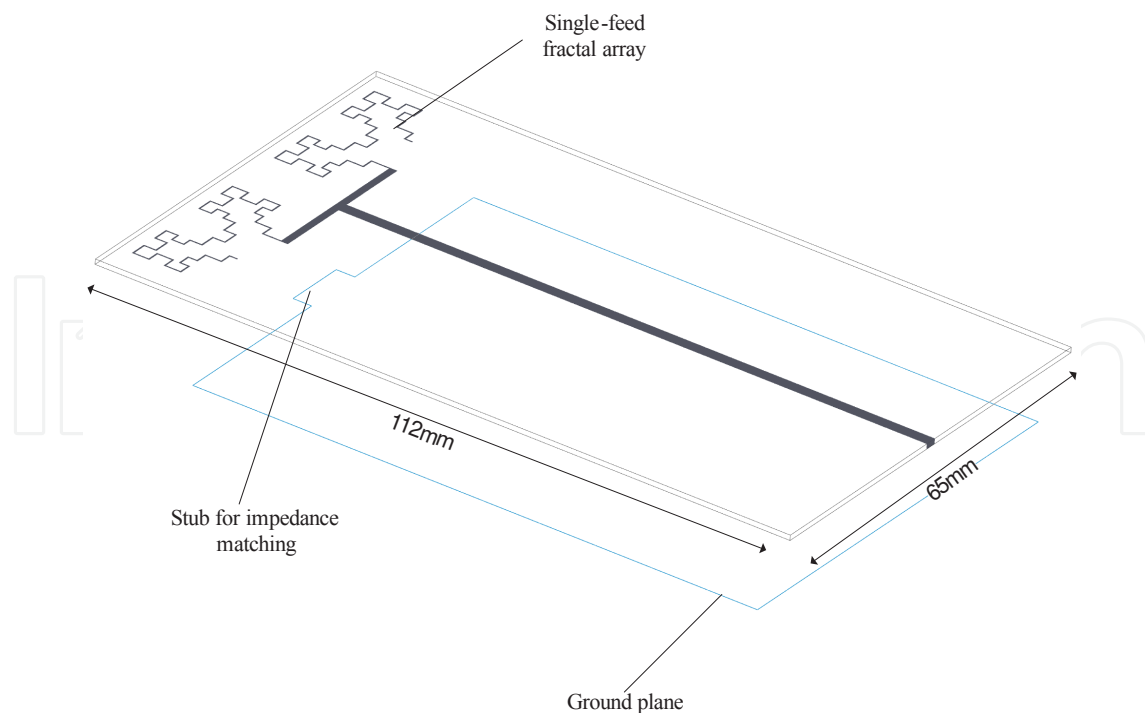
Figure 17. The single-feed fractal monopole array on a PDA size substrate proposed in [22]

As can be seen from Figure 17, on the top size of the partial ground plane, a rectangular stub is added. Without introducing the rectangular stub on the partial ground plane, it is found that the bandwidth of this antenna is not as good as expected: the bandwidth at the higher band (5 GHz) is quite narrow. Therefore, it is necessary to find a method to improve the bandwidth of the antenna at the higher band without affecting too much the resonant frequency at the lower band. Some common impedance matching methods such as quarter-wavelength transformer line or microstrip taper line, besides their large size, they are not suitable for this application, since they can only be applied to single band antennas. After several attempts, it was found that by adding a stub on the top edge of the ground plane, the impedance match of the antenna can be improved with little influence on the original resonant frequencies.

The improvement of the impedance matching of the proposed fractal antenna with the addition of a stub on the partial ground plane can be explained by modeling the stub as an equivalent L-Matching Network, as shown in Figure 18. The value of the inductance (L_1) and capacitance (C_1) at each resonant frequency is determined by the size/shape of the stub and the thickness/permittivity of the substrate. For the antenna presented in [22], due to the use of the fractal geometry, which has the advantage of self-affinity and exhibiting similar radiation character-istics at multiple resonant frequencies, the impedance matching was improved simultaneously at both resonant frequencies with the addition of an equivalent L-Network. This is one additional merit of employing fractals in monopole antenna design.
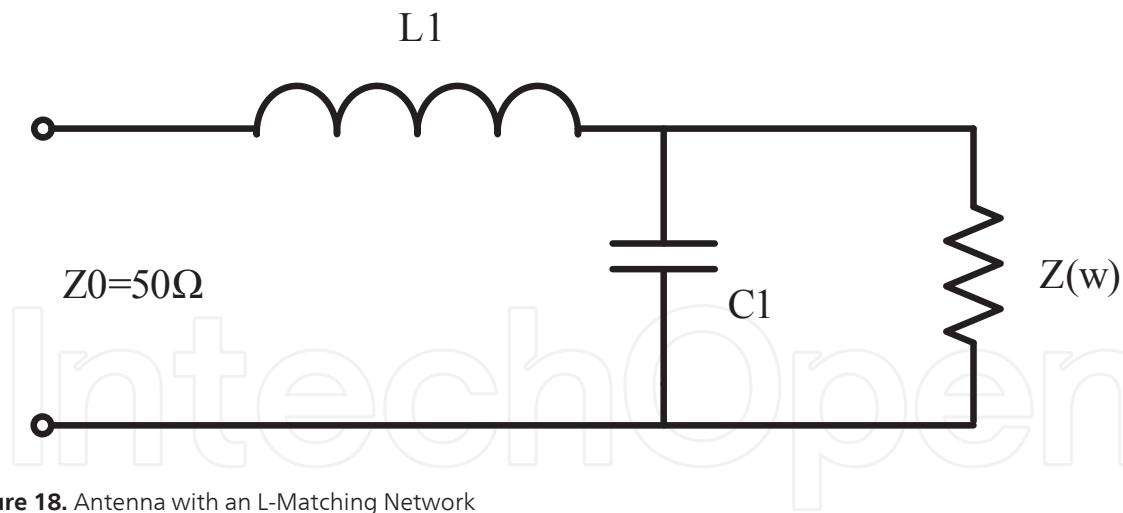
Figure 18. Antenna with an L-Matching Network

Figure 19 shows the measured and simulated reflection coefficient of this design. It can be observed that further optimization is required, to further increase the operating bandwidth of the antenna: it has a 10 dB bandwidth from 2.32 to 2.49 GHz and from 5.1 to 5.88 GHz, which covers the required 2.4, 5.2 and 5.8 GHz bands for 802.11a/b/g applications. Comparing the measured and simulated results, some frequency shifts were observed, which might be caused by the fabrication accuracy or the uncertainty of the dielectric constant of the substrate. By adjusting the size of the fractal geometry, the resonant frequencies can be easily tuned to the desired ones.
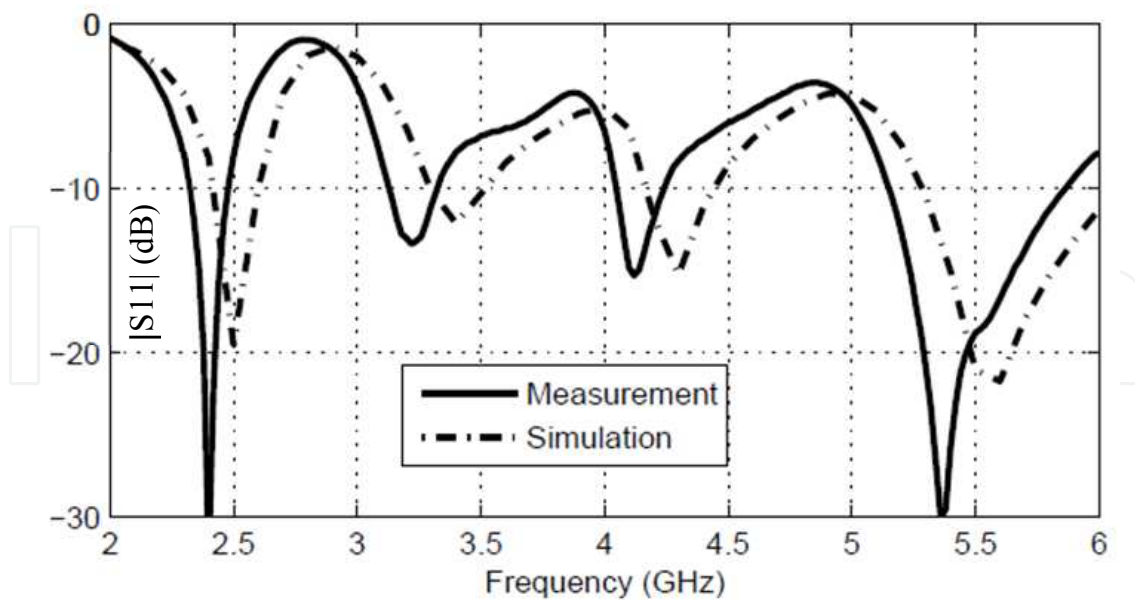
Figure 19. The measured and simulated S11 of the antenna array on a PDA size substrate [22]

The measured radiation patterns for this single-feed array show that at the lower band, the radiation pattern of this antenna array is similar to a normal printed monopole antenna, which has a isotropic radiation pattern at the H plane and two broadside radiation pattern at the E plane. In the upper band, the radiation patterns at both 5.2 and 5.8 GHz are more or less omnidirectional but there are some nulls in the E plane, which are due to the cancellation from the two radiation elements. The measurement results also indicate that the maximum gain of this printed monopole array can reach 2.3 dBi in the lower band and 5.6 dBi in the upper band. Compared to the case of a single radiation element, a minimum of 2 dB gain improvement has been achieved. Based on the simulation results, the radiation efficiency of this antenna array is 86% at 2.4 GHz, 82% at 5.2 GHz and 89% at 5.8 GHz.

### 4.2. Inverted-L antenna array for MIMO applications

Multiple-Input-Multiple-Output (MIMO) techniques enable a wireless device to transmit or receive data with higher data rate. The recently announced IEEE 802.11n and Long Term Evolution (LTE) standard requires the wireless LAN devices and mobile devices to support MIMO. The use of antenna arrays can improve the diversity performance of the antenna, which in turn increases the channel capacity by reducing the fading, suppressing both the random frequency modulation and co-channel interference. The biggest challenge in designing compact antenna arrays is how to maintain a good isolation between antennas that are closely spaced. To have good space diversity, traditionally the space between each antenna elements is required to be approximately half of the wavelength. However, for most of the commercial wireless devices, it is impossible to follow this rule due to the size constraints. The objective of this work is to explore solutions to design compact antenna arrays. The methodology adopted in this study employs the 'neutralizing technique'.

Designing a WLAN antenna for an USB dongle requires techniques for antenna miniaturization as the available volume left for the antenna is quite small compared to the wavelength at the required resonant frequency, which is quite challenging. As an example, in [23] a USB memory size antenna for 2.4 GHz Wireless LAN (WLAN) was achieved by using a folded trapezoidal antenna. In an USB dongle, the available volume for mounting the antennas is typically around $10 \times 17 \times 5$ mm³. With respect to the design of antenna arrays for USB dongles, it is a challenge task to improve the isolation between each antenna element, since the antennas have to be placed in close proximity. In [24], a dual band two antennas array was proposed. This antenna consists of an L-shape patch and a via trace connecting the via to the ground. To reach the expected performance, it needs precise fabrication and the experimental result shows that the isolation of this antenna array at 2.4 GHz is less than 9 dB. In [25], a MIMO antenna array for mobile WiMAX (3.5 GHz) was presented. This antenna has a 3D structure and the high isolation was achieved by using a common T-shaped ground plane. The disadvantages of this antenna array are that it is difficult to fabricate and the size of the ground plane can have a great effect on the radiation performance of the antenna due to the shorting structure. Regarding the design of compact planar antenna arrays for WLAN 5.8 GHz on a USB dongle, research has shown that there are few publications in this area, which is the main motivation behind this work. Recently, a new method named Neutralization Techniques has been proposed [26]. Using this method, the isolation of two Planar Inverted-F Antennas (PIFAs) can be improved through neutralizing the current of two antennas without the need of adding extra space for antenna design. So far, this method has only been applied in the design of PIFA antennas and there are few studies investigating the use of the neutralization technique. In this work, we further investigate this technique in the design of an Inverted-L antenna (ILA) array.

In [27], a compact and low cost Inverted-L antenna array is proposed for the MIMO application. Figure 20 shows the structure of a classic ILA. The ILA can be viewed as a bent monopole antenna and the total length of the inverted-L, L1+L2, needs to be approximately one quarter of wavelength at the resonant frequency of interest. However, the challenge of this work is that the two antennas need to be closely located in a small area of an USB dongle.
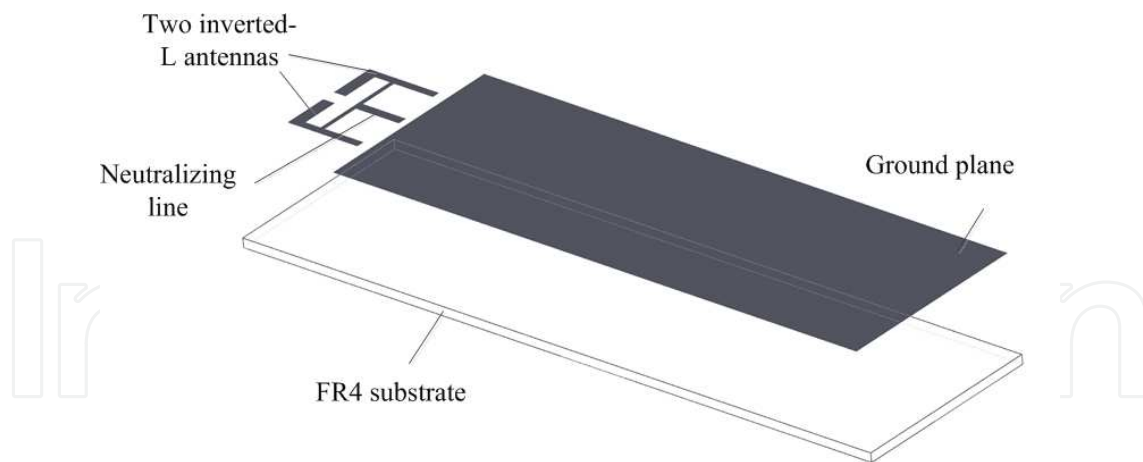
Figure 21 presents the structure of the proposed ILAs. The proposed antenna is fabricated on 0.8 mm thick FR4 with relative permittivity of 4.4 and loss tangent of 0.02. The distance between the two feeding points is $0.15\lambda_{5.8\text{GHz}}$ and the gap (d_1) between these two antennas is only $0.02\lambda_{5.8\text{GHz}}$, where $\lambda_{5.8\text{GHz}}$ represents the free space wavelength at 5.8 GHz. This antenna array has two equal ILAs that are located within a small distance on the PCB board of the USB dongle. Based on the concept proposed in [26], a neutralizing line is added between the two antenna elements to increase the isolation. The length of the neutralizing line is critical in determining the frequency band where the isolation between the two antenna ports can be improved. Increasing the length of the neutralizing line can make the antenna array to have good isolation at the lower frequency band. According to [26], the location of the neutralizing line needs to be placed where the surface current is maximum (minimum E field) and the length of it needs to be approximately a quarter wavelength.
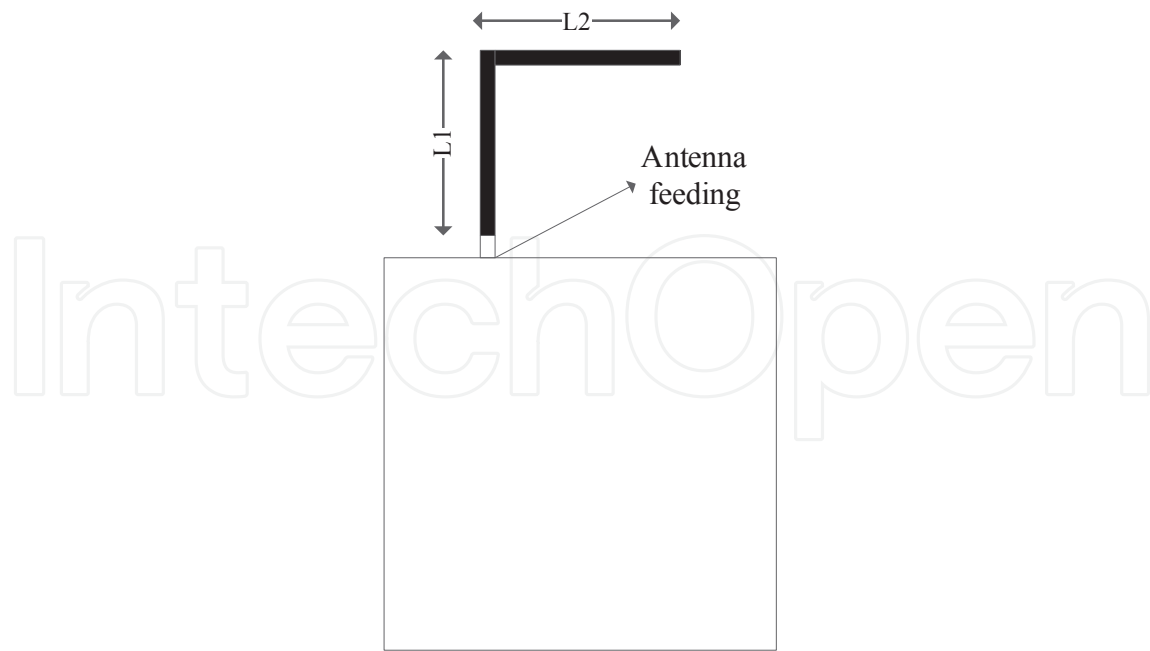
**Figure 20.** The structure of a typical Inverted-L antenna [27]

It is found in [27] that this antenna structure exhibits poor impedance matching at the desired frequency. The low input impedance of the ILA antenna is in fact one of its disadvantages [28]. The typical method employed to solve this problem for an ILA is to short the antenna element to the ground plane and change the feeding position, which in turn increases the input impedance of the antenna. Then the antenna becomes an Inverted-F antenna (IFA), whose input impedance is easier to be matched. However, shorting the antenna to the ground plane will increase the impact of the ground plane size to the radiation performance of the antenna. When connecting the USB dongle to a PC, for example, the equivalent size of the ground plane for the antenna is extended. In this scenario, the antenna may fail to operate at the desired frequency band. Moreover, the isolation between the antennas may also be influenced by shorting them to a common ground plane. Therefore, it is better to solve this limitation without resorting to short the antenna to the ground. Instead, the technique proposed in [27] improves the impedance matching of the antenna array by including one vertical stub in the middle of the neutralizing line, as depicted in Figure 21. From the aspect of the antenna array, where the isolation between the antennas is of concern, adding this stub has little influence on the isolation between the two antennas as the isolation is mainly controlled by the length, width and position of the horizontal neutralizing line. Meanwhile, for the single antenna itself, the equivalent antenna structure is one bent monopole with an L-shape stub, which operates as an impedance transformer.

Figure 22 shows the measured reflection coefficient and isolation of the proposed antenna array. The measurement results suggest that the proposed ILA array has a 10 dB return loss bandwidth from 5.7 to more than 6 GHz, which is more than the specification required for the WLAN 5.8 GHz frequency band of interest (5.725 to 5.875 GHz). This makes the performance of the proposed antenna more robust during product integration, such as immunity to

**Figure 21.** The structure of the proposed ILAs array in [27]

proximity to other components and the product enclosure, thus providing some margin against proximity effects which can lead to some frequency shifts. It is also found that the isolation between the two antennas is always better than 10 dB from 5.5 to 6.0 GHz and within the desired WLAN operation band, an isolation of 12 dB or more is obtained. It is observed that there is some frequency differences (less than 100 MHz) between the measured reflection coefficients of the two ports of the antenna array. This is due to the fabrication accuracy and soldering of the feeding cable, which results in the asymmetrical response of the two antenna elements. The measured results indicate that the proposed antenna array exhibits a maximum gain around 2.5 dBi at 5.8 GHz.
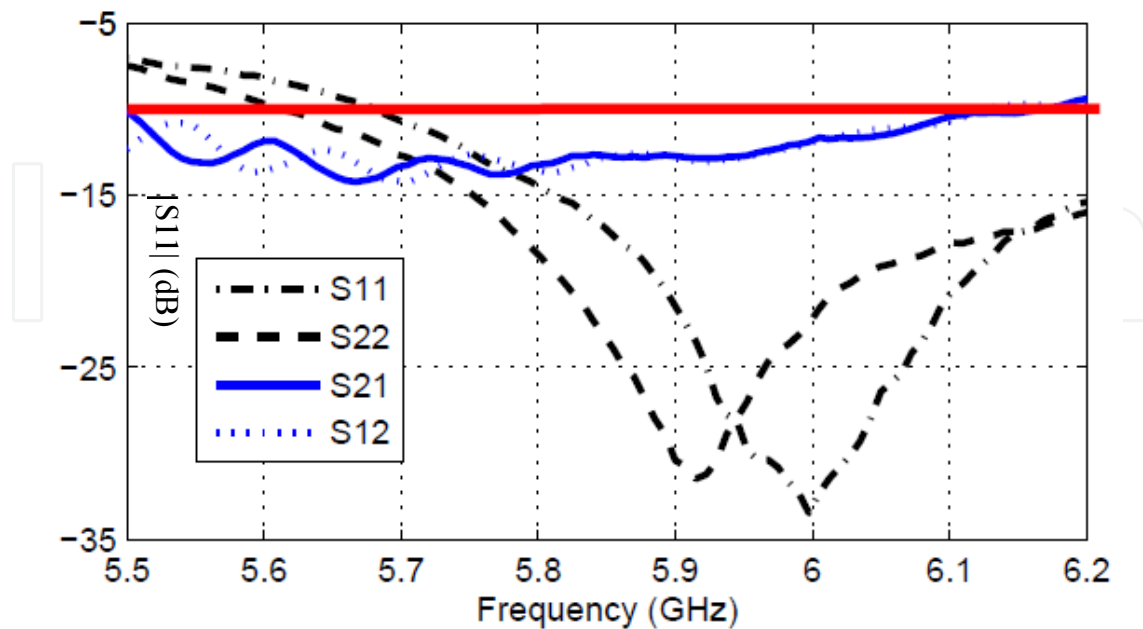
Figure 22. Measured reflection coefficient of the ILAs array proposed in [27]

5. Recent development

It has been shown in this chapter that the usage of two strips can contribute to the design of a dual band printed monopole. Recent research in [29] demonstrates that instead of using only two strips, a triple-band monopole can be designed using three strips. The structure of the triple-band printed monopole in presented in Figure 23. As seen, the printed monopole has three strips, each of which corresponds to a resonant frequency. This implies that introducing multiple strips, a multiband printed monopole can be obtained. This is one of the advantages of the printed monopole compared to other types of antennas. However, the difficulty of this approach lies in how to match the monopole at different resonant frequencies and reduce the influence from the mutual couplings between different strips.
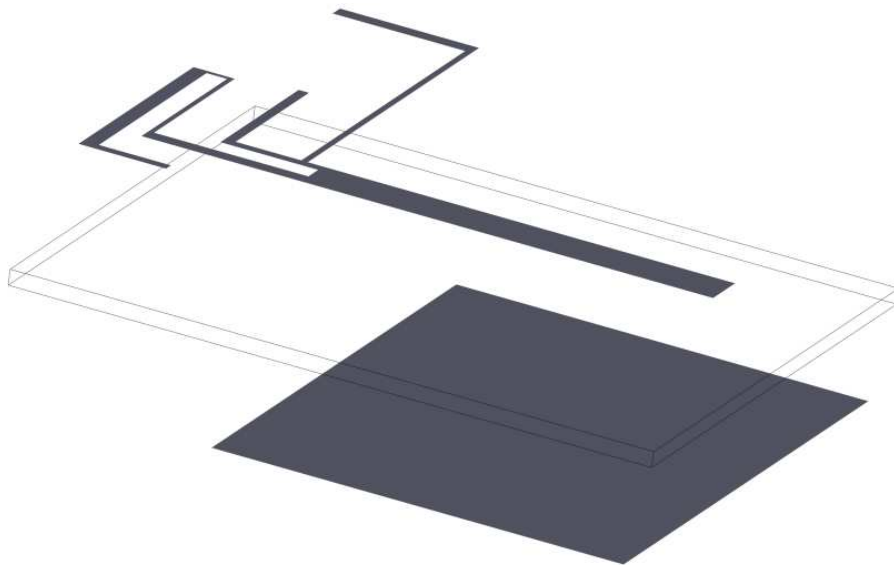

Figure 23. The proposed triple band printed monopole by [29]

It is also known that either using the meandered lines or the introduction a chip inductor can contribute to the size reduction of the monopole. Recently, a broadband LTE/WWAN antenna was designed for the tablet PC application [30]. This monopole is designed by employing both the meandered lines and chip inductor, thus greatly reducing the size of the antenna, whilst reaching a multiple frequency band operation. Similarly, a small printed monopole for DVB application is achieved by introducing a varactor on the meander line monopole [31]. By adding the varactor on the antenna radiating element, not only the antenna size is reduced, but also the frequency reconfigurablility can be achieved. Therefore, it can be concluded that combining different antenna miniaturization techniques to design a small printed monopole is an effective approach. Figure 24 demonstrates one example of introducing a lumped element on a meander line structure.
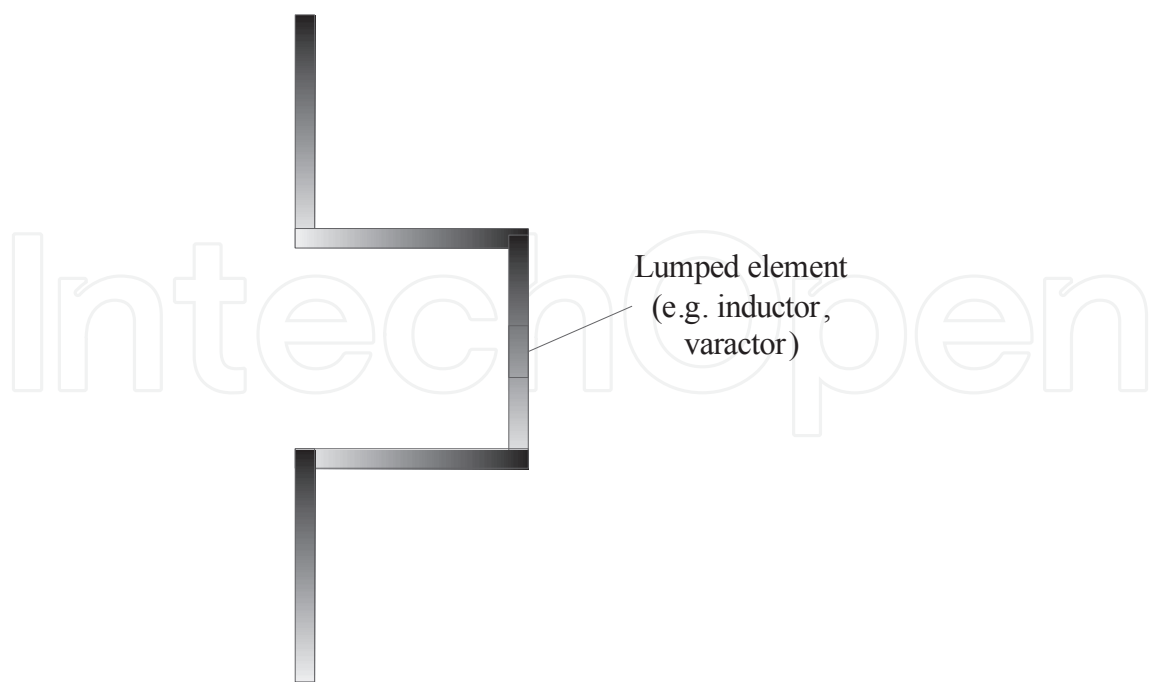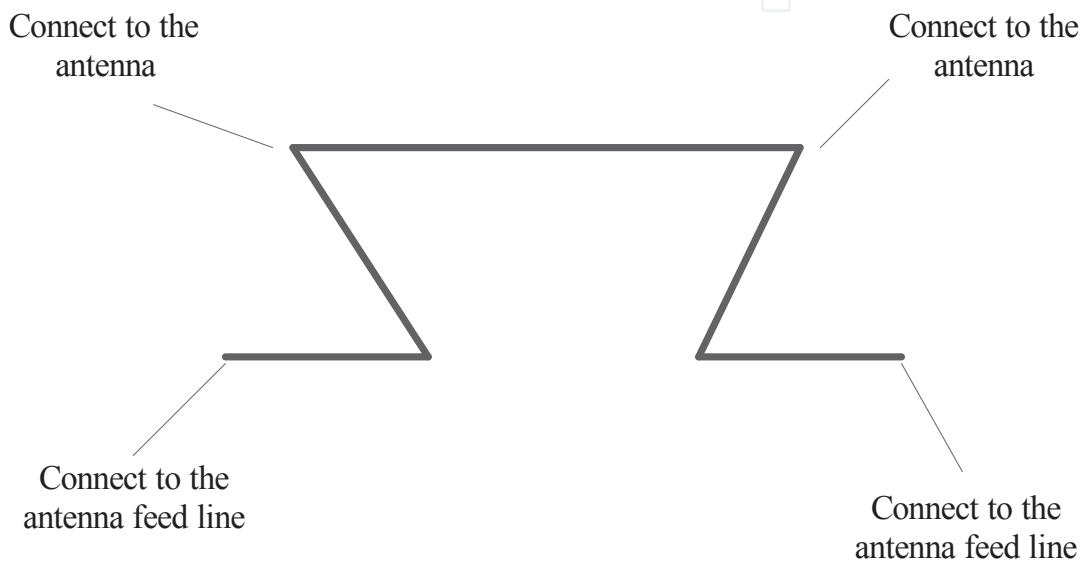
Figure 24. Demonstration of adding a lumped element on the meander line

To design a compact monopole array for the MIMO application, the key issue is to keep a high isolation between two or more radiating elements when they are closely spaced. The simulation results presented in [32] show that the orientation of the antenna elements can be critical in determining the isolation between the antennas. For example, with the spacing between two antennas elements of only one tenth of the wavelength, when the two monopoles are orthogonally oriented as the one shown in Figure 25, about 10-dB improvement in isolation can be observed. This can be explained by the polarization diversity. However, this approach will not be practical if a single polarization for the receiving signal is required to be used.
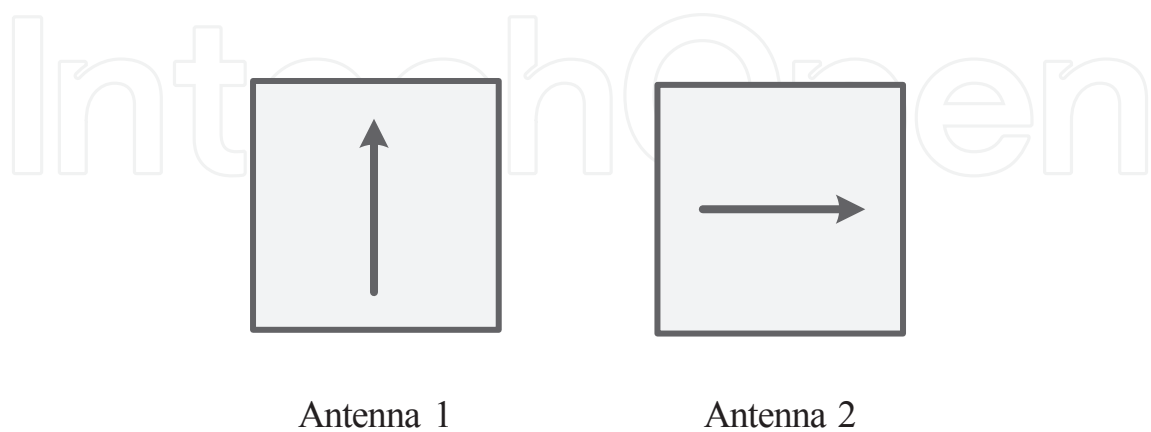
Figure 25. Example of placing two antennas in orthogonal position

Recently, a new approach based on the neutralizing technique, which has been introduced in this chapter, is proposed in [33]. Figure 26 shows the configuration of the neutralizing line. In this approach,a high isolation over a wideband frequency is reached by creating four current paths between the two antenna elements, which is achieved by attaching the neutralizing line to both the antenna elements and the feed line at its maximum current position. The measurement results provided in [33] show that this is an effective method to design a compact wideband printed monopole array for MIMO applications. This constitutes a further development for the conventional neutralizing technique proposed by [26].

Connect to the antenna

Connect to the antenna

Connect to the antenna feed line

Connect to the antenna feed line

Figure 26. The modified the neutralizing line proposed in [31]

6. Conclusion

In this chapter, several techniques that can be employed to design compact and low cost printed monopole antennas and antenna arrays have been introduced. Either using some special geometry (e.g. fractals) or introducing lumped elements on the radiating elements, multiband monopole with reduced size can be implemented. The recent studies also show that combining both methods, additional size reduction can be achieved. However, the disadvantage is that the antenna radiation performance will be influenced. In the field of compact printed monopole arrays, the use of the neutralizing technique has been proved to be an effective method that can be applied to the planar monopole design, which can result in a simple and low cost solution. To reach a wideband operation, the modified neutralizing line proposed in [31] provides a good solution.

Author details

Qi Luo[1], Jose Rocha Pereira[2,3] and Henrique Salgado[4,5]

1 School of Engineering and Digital Arts, University of Kent, Canterbury, UK

2 University of Aveiro, Portugal

3 Instituto de Telecomunicações, Aveiro, Portugal

4 Faculdade de Engenharia Universidade do Porto, Porto, Portugal

5 INESC TEC - Instituto de Engenharia de Sistemas e Computadores do Porto, Porto, Portugal

References

[1] L. J. Chu, "Physical Limitations of Omni-Directional Antennas," *Journal of Applied Physics,* vol. 19, no. 12, pp. 1163-1175, 1948.

[2] B. B. Mandelbrot, *The fractal geometry of nature*, Updated and augm. ed., New York: W.H. Freeman, 1983.

[3] Q.Luo, "Design synthesis and miniaturization of multiband and reconfigurable microstrip antenna for future wireless applications," University of Porto, 2014.

[4] Q. Luo, H. M. Salgado, and J. R. Pereira, "Fractal Monopole Antenna Design Using Minkowski Island Geometry," *2009 Ieee Antennas and Propagation Society International Symposium and Usnc/Ursi National Radio Science Meeting, Vols 1-6*, pp. 2639-2642, 2009.

[5] Q. Luo, J. R. Pereira, and H. M. Salgado, *Inverted-L Antenna (ILA) Design Using Fractal for WLAN USB Dongle*, 2013.

[6] N. Cohen, "Fractal antenna applications in wireless telecommunications." pp. 43-49.

[7] Q. Luo, J. R. Pereira, and H. M. Salgado, "Compact Printed Monopole Antenna With Chip Inductor for WLAN," *Ieee Antennas and Wireless Propagation Letters,* vol. 10, pp. 880-883, 2011.

[8] A. D. Yaghjian, and S. R. Best, "Impedance, bandwidth, and Q of antennas," *Antennas and Propagation, IEEE Transactions on,* vol. 53, no. 4, pp. 1298-1324, 2005.

[9] K. L. Wong, and C. H. Huang, "Compact multiband PIFA with a coupling feed for internal mobile phone antenna," *Microwave and Optical Technology Letters,* vol. 50, no. 10, pp. 2487-2491, Oct, 2008.

[10] C. H. Chang, K. L. Wong, and J. S. Row, "Coupled-Fed Small-Size Pifa for Penta-Band Folder-Type Mobile Phone Application," *Microwave and Optical Technology Letters,* vol. 51, no. 1, pp. 18-23, Jan, 2009.

[11] C. I. Lin, and K. L. Wong, "Printed monopole slot antenna for penta-band operation in the folder-type mobile phone," *Microwave and Optical Technology Letters,* vol. 50, no. 9, pp. 2237-2242, Sep, 2008.

[12] F. H. Chu, and K. L. Wong, "Simple Folded Monopole Slot Antenna for Penta-Band Clamshell Mobile Phone Application," *Ieee Transactions on Antennas and Propagation,* vol. 57, no. 11, pp. 3680-3684, Nov, 2009.

[13] K. L. Wong, and C. H. Huang, "Printed loop antenna with a perpendicular feed for penta-band mobile phone application," *Ieee Transactions on Antennas and Propagation,* vol. 56, no. 7, pp. 2138-2141, Jul, 2008.

[14] C. I. Lin, and K. L. Wong, "Internal meandered loop antenna for GSM/DCS/PCS multiband operation in a mobile phone with the user's hand," *Microwave and Optical Technology Letters,* vol. 49, no. 4, pp. 759-765, Apr, 2007.

[15] Y. W. Chi, and K. L. Wong, "Half-wavelength loop strip capacitively fed by a printed monopole for penta-band mobile phone antenna," *Microwave and Optical Technology Letters,* vol. 50, no. 10, pp. 2549-2554, Oct, 2008.

[16] P. Ciais, R. Staraj, G. Kossiavas *et al.,* "Compact internal multiband antenna for mobile phone and WLAN standards," *Electronics Letters,* vol. 40, no. 15, pp. 920-921, Jul 22, 2004.

[17] C. I. Lin, and K. L. Wong, "Printed monopole slot antenna for internal multiband mobile phone antenna," *Ieee Transactions on Antennas and Propagation,* vol. 55, no. 12, pp. 3690-3697, Dec, 2007.

[18] H. Hsuan-Wei, L. Yi-Chieh, T. Kwong-Kau *et al.,* "Design of a Multiband Antenna for Mobile Handset Operations," *Antennas and Wireless Propagation Letters, IEEE,* vol. 8, pp. 200-203, 2009.

[19] A. C. K. Mak, C. R. Rowell, R. D. Murch *et al.,* "Reconfigurable Multiband Antenna Designs for Wireless Communication Devices," *Antennas and Propagation, IEEE Transactions on,* vol. 55, no. 7, pp. 1919-1928, 2007.

[20] J. K. Ji, G. H. Kim, and W. M. Seong, "A Compact Multiband Antenna Based on DNG ZOR for Wireless Mobile System," *Ieee Antennas and Wireless Propagation Letters,* vol. 8, pp. 920-923, 2009.

[21] K. L. Wong, and S. C. Chen, "Printed Single-Strip Monopole Using a Chip Inductor for Penta-Band WWAN Operation in the Mobile Phone," *Ieee Transactions on Antennas and Propagation,* vol. 58, no. 3, pp. 1011-1014, Mar, 2010.

[22] L. Qi, H. M. Salgado, and J. R. Pereira, "Printed fractal monopole antenna array for WLAN." pp. 1-4.

[23] K. Sekine, and H. Iwasaki, "USB Memory Size Antenna for 2.4 GHz Wireless LAN and UWB." pp. 1173-1176.

[24] A. Gummalla, M. Achour, G. Poilasne *et al.*, "Compact Dual-Band Planar Metamaterial Antenna Arrays for Wireless Lan," *2008 Ieee Antennas and Propagation Society International Symposium, Vols 1-9*, pp. 4595-4598, 2008.

[25] K. Jaesoon, K. Dongho, L. Youngki *et al.*, "Design of a MIMO antenna for USB dongle application using common grounding." pp. 313-316.

[26] C. Luxey, "Design of multi-antenna systems for UMTS mobile phones." pp. 57-64.

[27] L. Qi, C. Quigley, J. R. Pereira *et al.*, "Inverted-L antennas array in a wireless USB dongle for MIMO application." pp. 1909-1912.

[28] Z. N. Chen, "Note on impedance characteristics of L-shaped wire monopole antenna," *Microwave and Optical Technology Letters,* vol. 26, no. 1, pp. 22-23, 2000.

[29] C. H. Ku, L. K. Li, and W. L. Mao, "Compact Monopole Antenna with Branch Strips for Wlan/Wimax Operation," *Microwave and Optical Technology Letters,* vol. 52, no. 8, pp. 1858-1861, Aug, 2010.

[30] S. H. Chang, and W. J. Liao, "A Broadband LTE/WWAN Antenna Design for Tablet PC," *Ieee Transactions on Antennas and Propagation*, vol. 60, no. 9, pp. 4354-4359, Sep, 2012.

[31] M. Komulainen, M. Berg, H. Jantunen *et al.*, "Compact varactor-tuned meander line monopole antenna for DVB-H signal reception," *Electronics Letters,* vol. 43, no. 24, pp. 1324-1326, 2007.

[32] H. F. Abutarboush, R. Nilavalan, S. W. Cheung *et al.*, "Compact Printed Multiband Antenna With Independent Setting Suitable for Fixed and Reconfigurable Wireless Communication Systems," *Ieee Transactions on Antennas and Propagation*, vol. 60, no. 8, pp. 3867-3874, Aug, 2012.

[33] C. H. See, R. A. Abd-Alhameed, Z. Z. Abidin *et al.*, "Wideband Printed MIMO/Diversity Monopole Antenna for WiFi/WiMAX Applications," *Ieee Transactions on Antennas and Propagation*, vol. 60, no. 4, pp. 2028-2035, Apr, 2012.